



# HHS Public Access

Author manuscript

*Bioorg Chem.* Author manuscript; available in PMC 2021 March 01.

Published in final edited form as:

*Bioorg Chem.* 2020 March ; 96: 103585. doi:10.1016/j.bioorg.2020.103585.

## Efficient Synthesis of NIR Emitting Bis[2-(2'-hydroxyphenyl)benzoxazole] Derivative and Its Potential for Imaging Applications

Junfeng Wang<sup>a,c,d</sup>, Hannah Baumann<sup>a</sup>, Xiaoman Bi<sup>a</sup>, Leah P. Shriver<sup>a</sup>, Zhaoda Zhang<sup>d</sup>, Yi Pang<sup>\*,a,b</sup>

<sup>a</sup>Department of Chemistry, The University of Akron, Akron, OH, USA, 44325

<sup>b</sup>Maurice Morton Institute of Polymer Science, The University of Akron, Akron, OH, USA, 44325

<sup>c</sup>Gordon Center for Medical Imaging, Massachusetts General Hospital and Harvard Medical School, 125 Nashua Street, Boston, MA, 02114

<sup>d</sup>Martinos Center for Biomedical Imaging, Massachusetts General Hospital and Harvard Medical School, 149, 13<sup>th</sup> st, Charlestown, MA, 02129

### Abstract

Unassymmetric bis[2-(2'-hydroxyphenyl)benzoxazole] bis(HBO) derivatives with a DPA functionality for zinc binding have been developed with an efficient synthetic route, using the retrosynthetic analysis. Comparison of bis(HBO) derivatives with different substitution patterns allows us to verify and optimize their unique fluorescence properties. Upon binding zinc cation, bis(HBO) derivatives give a large fluorescence turn-on in both visible ( $\lambda_{em} \approx 536$  nm) and near-infrared (NIR) window ( $\lambda_{em} \approx 746$  nm). The probes are readily excitable by a 488 nm laser, making this series of compounds a suitable imaging tool for *in vitro* and *in vivo* study on a confocal microscope. The application of zinc binding-induced fluorescence turn-on is successfully demonstrated in cellular environments and thrombus imaging.

### Graphics Abstract

---

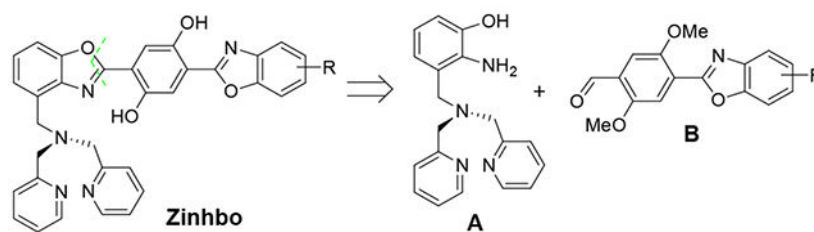
\* yp5@uakron.edu.

**Publisher's Disclaimer:** This is a PDF file of an unedited manuscript that has been accepted for publication. As a service to our customers we are providing this early version of the manuscript. The manuscript will undergo copyediting, typesetting, and review of the resulting proof before it is published in its final form. Please note that during the production process errors may be discovered which could affect the content, and all legal disclaimers that apply to the journal pertain.

#### Declaration of interests

The authors declare that they have no known competing financial interests or personal relationships that could have appeared to influence the work reported in this paper.

Appendix A. Supplementary data associated with this article can be found in the online version at <https://doi.org/10.1016/j.bioorg.2020.103585>.



An efficient synthesis route is found to give Zinhbo compounds that give NIR-emission upon binding  $Zn^{2+}$  in cellular environments.

## Keywords

Fluorescent probe; Near Infrared; Benzoxazole; ESIPT; Zinc; Thrombus imaging

## Introduction

In recent years, fluorescent sensors are emerging as powerful tools for molecular imaging.<sup>1</sup> In this attractive field, there are increasing interests to develop optical probes that give emission in the near-infrared (NIR) region (650-900 nm). This is because the NIR photons can penetrate deeply through biological tissues, thereby enabling detection of molecular activity for *in vivo* applications.<sup>2-7</sup> An ideal NIR probe should also exhibit a large Stokes' shift, in order to have minimum interference between excitation and emission signals. Additionally, a qualified NIR probe should be integrated with a suitable chemical event that can generate a large optical response when responding to a specific analyte of interest.<sup>8</sup>

2-(2'-Hydroxyphenyl)benzoxazole (HBO) derivatives represent an interesting class of dyes, which exhibit a large Stokes' shift (> 150 nm) arising from the excited-state intramolecular proton transfer (ESIPT).<sup>9,10</sup> The photochemical event is dependent on the presence of the phenolic proton, whose migration to the "nitrogen" allows the formation of its corresponding *keto* tautomer with emission at a longer wavelength. The metal chelation to mono HBO system, however, removes the phenolic proton, thereby eliminating the ESIPT.<sup>11,12</sup> In an effort to overcome the barrier and enable the ESIPT from a metal-HBO complex, we recently showed that 2, 5-bis(benzoxazole-2-yl)benzene-1,4-diol derivatives **1**, bis(HBO), can exhibit a remarkable optical response upon zinc binding, giving the turn-on emission in both visible (at ~550 nm) and NIR regions (at ~750 nm).<sup>13-15</sup> The chemical event for the sensor response is dependent on the formation of **2**, where the zinc complexation acts as an effective switch to turn-on the ESIPT emission (corresponding to the emission in NIR region). In the molecular design of **1**, a 2, 2'-dipicolylamine (DPA) group is attached to selectively bind  $Zn^{2+}$  cation, while a remaining HBO is used to enable the ESIPT. The choice of DPA ligand is based on its high selectivity to  $Zn^{2+}$  cation. Despite the impressive sensor performance of **1b** (low toxicity and large response to  $Zn^{2+}$  binding),<sup>15</sup> the synthesis of **1** suffers from low yields, which hamper its broad application. The previous synthesis was based on a linear *consecutive* sequence consisting of 8 steps,<sup>15,16</sup> which makes it difficult to access this class of compounds for extensive studies. In an continuing effort to overcome the barrier, we now report a highly efficient synthesis of 2, 5-

bis(HBO) derivatives with a DPA functionality, by adopting a *convergent* synthetic strategy. In the synthesis design, the target molecule was disconnected in the middle to give two fragments **A** and **B** (Scheme 1), thereby leading to improved yields.

In the previous synthesis of **1b**,<sup>15</sup> the low yield was associated with the introduction of the DPA group, which was accomplished by using a sequence of low-yielding reactions to accomplish the transformation  $\text{Ar-CH}_3 \rightarrow \text{Ar-CH}_2\text{-N}(\text{CH}_2\text{-py})_2$ . Although an improved methodology was developed to synthesize Zinhbo compounds with higher yields, the reduction of the carboxylic ester group in the synthesis greatly limited the diversity of these derivatives.<sup>16</sup> Herein we report a new strategy for efficient synthesis of bis(HBO) derivatives, which is based on a retrosynthetic analysis involving the bond disconnections in the middle of the target to give two fragments **A** and **B** (Scheme 1). The synthetic direction can be outlined as follows: (1) preparation of the key intermediate **A**, which incorporates the DPA group in the early stage; (2) efficient synthesis of benzoxazole **B** from aldehyde **C** and 2-amino-phenol **D**; (3) reaction of **A** and **B** to give the bis(HBO) products

## Results and Discussion

Scheme 2 presents the construction of the key intermediate **A**. Thus compound **5** was prepared conveniently by the nitration of **4** with nitric acid at room temperature, which precipitated from the solution and was recrystallized from EtOAc/hexane as large colorless crystals (50-60% yield). Selective reduction of ester **5** by  $\text{NaBH}_4$  in THF/MeOH<sup>17,18</sup> proceeded cleanly to furnish alcohol **6**, which then underwent tosylation or bromination to provide corresponding **7** or **8** in almost quantitative yields.<sup>19,20</sup> Reaction of **7** or **8** with 2, 2'-dipicolylamine (DPA) in the presence of  $\text{K}_2\text{CO}_3$  and KI gave compound **9** in good yields.<sup>21</sup> Deprotection of the methoxy group proceeded smoothly at room temperature by using  $\text{AlCl}_3$  to give **10**,<sup>22</sup> which was then reduced by  $\text{H}_2$  over Pd/C to afford the intermediate **A** in almost quantitative yield. Although the procedure was quite satisfactory on a small scale (e.g., 1 mmol), the deprotection of **9** by  $\text{AlCl}_3$  was found to be troublesome for a larger scale reaction (e.g., 5 mmol). The reaction was not completed even by using a large excess of  $\text{AlCl}_3$ . This is because some syrup-like residues precipitated out during the reaction, possibly due to (a) chelation of  $\text{AlCl}_3$  with DPA, and (b) encapsulation of unreacted **9**. In order to overcome the deficiency in the deprotection of **9**, our attention was directed to seek deprotection of the methyl phenol ether at an earlier stage, i.e. before introduction of DPA. Attempts to deprotect the methyl from the phenol ether **6** gave low yield by using either  $\text{AlCl}_3$  or  $\text{BBr}_3$ . However, the methyl group of **8** was removed effectively by using  $\text{AlCl}_3$  to give 3-(bromomethyl)-2-nitrophenol, which could be converted to **10** in high yield.

The construction of the benzoxazole fragment **B** from intermediate **C** and 2-aminophenols **D** (Scheme 3) was also significantly improved with a one-pot reaction. In the synthesis of benzoxazole compounds, most reported methods require the isolation of the imine intermediate **11**, followed by an oxidative cyclization to form the benzoxazole intermediate **12**.<sup>23-29</sup> Although DDQ and  $\text{Pb}(\text{OAc})_4$  worked well for oxidative cyclization of **11**,<sup>13-15</sup> the reaction typically gave the alcohol **12** without further oxidation. An additional oxidation step was thus required to further oxidize the alcohol **12** with another oxidant, in order to obtain the aldehyde **B**. In other words, the reaction sequence  $\mathbf{11} \rightarrow \mathbf{12} \rightarrow \mathbf{B}$  could be accomplished by

involving two steps of oxidation. An intriguing question is whether one can find a suitable oxidant that can execute both “oxidative cyclization” and “oxidation of the alcohol to the aldehyde”, thereby greatly simplifying the reaction procedure. Bearing this in mind, we decided to examine PCC which is known to oxidize primary alcohols to aldehydes and to oxidize imine to benzoxazoles as well.<sup>30</sup> Simple mixing of **C** and **D** with PCC in CH<sub>2</sub>Cl<sub>2</sub> led to **B** in 26% yield, and a large amount of byproduct was identified as **13**. The initial result indicated that PCC was effective for both cyclization and oxidation. Interestingly, when using TLC to monitor the reaction, we found **C** and **D** reacted quickly on TLC plate, forming imine intermediate **11**. This observation encouraged us to optimize the reaction conditions with silica gel and PCC. After extensive trials, a *one-pot* multistep method for the synthesis of **B** (by direct reaction between **C** and **D**) was developed in 60-80% yield with high reproducibility by silica gel and PCC.

Finally, the coupling of **A** and **B** was studied (Scheme 4). Unfortunately, all the reported catalysts and reagents such as Mn(OAc)<sub>3</sub>,<sup>26</sup> KAl(SO<sub>4</sub>)<sub>2</sub>,<sup>27</sup> Pb(OAc)<sub>4</sub>,<sup>28</sup> Ba(MnO<sub>4</sub>)<sub>2</sub>,<sup>29</sup> DDQ and even the PCC/silica gel method failed to give any desirable **15** (Scheme 4). It was found that the imine **14** was not formed by refluxing **A** and **B** in EtOH or toluene overnight, probably due to the steric hindrance. After exhaustive exploration, fortunately, we found that Tagawa’s method using O<sub>2</sub> with activated carbon gave **15** in up to 72% yield.<sup>31</sup> The final product **1b** could be easily prepared by the deprotection of methoxy groups catalyzed by AlCl<sub>3</sub> or BBr<sub>3</sub> in anhydrous CH<sub>2</sub>Cl<sub>2</sub>. With the availability of the intermediate **A**, the products (**1b-1d**) could be effectively synthesized in 2 steps in high yields.

### Fluorescent properties and imaging application

The newly developed synthetic strategy allowed us to obtain Zinhbo-6 and Zinhbo-7, in addition to the previously reported Zinhbo-1<sup>13</sup> and Zinhbo-5.<sup>15</sup> Optical properties of these Zinhbo compounds (Scheme 5) allowed us to examine the possible substituent effect. Fluorescence spectra of these Zinhbo compounds revealed one emission peak ( $\lambda_{em} \approx 607$  nm) (Figure 2). Upon binding Zn<sup>2+</sup>, the resulting Zinhbo-Zn<sup>2+</sup> complexes gave two characteristic emission peaks ( $\lambda_{em} \approx 536, 746$  nm), corresponding to their *enol* and *keto* tautomers (**2** and **3**, respectively). The ability of using Zn<sup>2+</sup> binding to generate two well separated emission is a unique property of Zinhbo compounds. In the study, one fundamental question is how the structure can be modified to affect the NIR emission wavelength and its intensity. In order to make comparison, the fluorescence spectra were normalized at the green emission peak ( $\lambda_{em} \approx 536$ , Figure 2). The alkyl substituent on 4-, 5-, and 6-position exhibited essentially no effect on the emission wavelength. However, the positions of alkyl substituents significantly influenced the relative NIR emission intensity, which could be attributed to the electronic perturbation by the substituents. The position of the alkyl substituents was found to affect not only the NIR emission, but also the quantum yield (ESI, Table S1). However, Zinhbo-5 remained to be the best among them in terms of the strong NIR emission (Figure 2 and ESI, Figure S2).

The ability of Zinhbo-5 to give simultaneous emission in both green and NIR channels, when responding to Zn<sup>2+</sup> binding,<sup>15</sup> encouraged us to use the probe on confocal microscope study, which has not been examined before. Since the probe-Zn<sup>2+</sup> complex can be excited

readily by a 488 nm laser, it would be a useful tool for imaging exogenous and endogenous  $Zn^{2+}$  ions in living cells (Figure 3). Thus, HeLa cells were stained with Zinhbo-5 (10  $\mu M$ ) in culture medium with prolonged incubation time (60 min) at 37°C, we were delighted to find observable green and NIR signal, which reveals the great sensitivity of this sensor. With exogenous  $Zn^{2+}$  ions (10  $\mu M$ ), very strong green and NIR signals were obtained on the confocal image throughout the cytoplasm. This further proved the great sensitivity and biocompatibility of the sensor. As far as we know, this is the first successful *in vitro* zinc selective NIR turn-on imaging with ESIPT property (> 270 nm Stokes' shift).

In order to examine the probe's general utility, Zinhbo-5 was further used to stain oligodendrocytes that are myelinating glial cells of the central nervous system. Thus, to the MO3.13 cells media (oligodendrocytes) were treated with TPEN (*N,N,N',N'*-tetrakis(2-pyridylmethyl)ethylenediamine) that is a high-affinity zinc chelator, washed with cell medium and added Zinhbo-5 (5  $\mu M$ ). The fluorescence confocal imaging revealed that Zinhbo-5 readily stained the cells (Figure 4). While the fluorescence signal of Zinhbo-5 was very weak in the absence of  $Zn^{2+}$  (Figure 4d), addition of  $Zn^{2+}$  induced a large fluorescence turn-on (Figure 4e and 4f). Similar results were also obtained when staining Fibroblast cells. These results illustrated that Zinhbo-5 could be a useful probe for monitoring cellular zinc level.

Cell viability of **Zinhbo-5** was checked with HEK293 cells in DMEM medium, by using alamar blue assay. No significant cell toxicity was observed up to 48 hours of the cells with up to 100  $\mu M$  concentration, when the DMSO stock solution (10 mM) was diluted to cell culture medium (ESI Figure S5). The ability of Zinhbo-5 in responding to cellular  $Zn^{2+}$ , in addition to its low toxicity, encouraged us to seek its further application. An interesting problem is blood clot, which is formed when responding to the blood vessel injury (e.g. resulting from cuts and bruises) in order to prevent bleeding. However, blood clot in the absence of injury (called thrombus) can be dangerous, as it can block a key blood vessel to impede blood flow, leading to cardiovascular diseases such as heart attack, stroke, pulmonary embolism, and deep vein thrombosis. It is known that zinc is involved in thrombosis and thrombolysis, where  $Zn^{2+}$  concentration is delicately controlled in the blood.<sup>32</sup> When  $Zn^{2+}$  cations circulate in plasma at a concentration of 10–20  $\mu M$ , most cations are bound to plasma proteins such as albumin (forming a labile, exchangeable pool), but some (about 0.1–2  $\mu M$ ) are in a free unbound state. Because the platelets in thrombi, which respond to blood vessel damage, are 50-100 folds higher than those found in the circulating blood. Upon activation,  $Zn^{2+}$  stored in platelets are released, thereby increasing the free zinc concentrations.<sup>32–37</sup> Therefore, the high  $Zn^{2+}$  concentrations in thrombus may enable the zinc sensors for thrombus imaging. To test this hypothesis, the *in vitro* blood clot model was generated by addition of thrombin into the human plasma according to a reported protocol.<sup>38</sup> The clear blood clots could be seen within 10-15 min (Figure 5, right well of top row). The significant fluorescence turn-on signals within the clots were displayed in both green and NIR channel (Figure 5, right well). There was no fluorescence signal generated by Zinhbo-5 in the plasma (Figure 5, left well). This result demonstrates that the NIR fluorescence zinc turn-on dyes such as Zinhbo-5 are promising probes for thrombus imaging. To our best knowledge, this is the first thrombus imaging evidenced by an NIR zinc sensor.

In summary, an efficient synthetic route has been developed for the synthesis of bis(HBO) compounds with the zinc-chelating DPA functionality. When using together with silica gel, PCC is found to be effective for accomplishing both “oxidative cyclization” and “oxidation of alcohol” steps, thereby greatly simplifying the reaction sequence. The finding opens a path to access this class of compounds for imaging applications, which are known to exhibit low toxicity and attractive fluorescence<sup>15</sup> but are rather difficult to synthesize. The availability of the bis(HBO) sensor **1** allows us to further examine its potential imaging applications for zinc detection, since it exhibits attractive photophysical properties including large fluorescence turn-on in the desirable NIR region upon zinc binding. The successful *in vitro* NIR imaging for the detection of exogenous and endogenous Zn<sup>2+</sup> ions in living cells makes this sensor a promising tool for imaging applications. This is further demonstrated by observing significant fluorescence turn-on signals within the blood clots. Study by using the improved synthesis to access other new NIR-emitting zinc sensors is in progress, and their potential applications for imaging zinc-related disease/diagnosis will be reported in another forthcoming manuscript.

## Supplementary Material

Refer to Web version on PubMed Central for supplementary material.

## Acknowledgements.

YP acknowledge support from Coleman endowment (from the University of Akron) and National Institute of Health (Grant No: 1R15GM126438-01A1) and ZZ acknowledge support from NIH National Cancer Institute (NCI) (Grant No: 1R01CA197401).

## References

1. Goncalves MS Fluorescent Labeling of Biomolecules with Organic Probes. *Chem. Rev* 2009, 109, 190–212. [PubMed: 19105748]
2. Guo Z; Park S; Yoon J; Shin I Recent progress in the development of near-infrared fluorescent probes for bioimaging applications. *Chem. Soc. Rev* 2014, 43, 16–29. [PubMed: 24052190]
3. Bremer C; Tung CH; Bogdanov A; Weissleder R Imaging of Differential Protease Expression in Breast Cancers for Detection of Aggressive Tumor Phenotypes. *Radiology* 2002, 222, 814–818. [PubMed: 11867806]
4. Kiyose K; Kojima H; Nagano T Functional Near-Infrared Fluorescent Probes. *Chem. Asian J* 2008, 3 (3), 506–515.
5. Licha K; Olbrich C Optical imaging in drug discovery and diagnostic applications. *Adv. Drug Delivery Rev* 2005, 57 (8), 1087–1108.
6. Ntziachristos V; Bremer C; Weissleder R Fluorescence imaging with near-infrared light: new technological advances that enable *in vivo* molecular imaging. *Eur. Radiology* 2003, 13, 195–208.
7. Oshiki D; Kojima H; Terai T; Arita M; Hanaoka K; Urano Y; Nagano T Development and Application of a Near-Infrared Fluorescence Probe for Oxidative Stress Based on Differential Reactivity of Linked Cyanine Dyes. *J. Am. Chem. Soc* 2010, 132, 2795–2801. [PubMed: 20136129]
8. Luo SL; Zhang EL; Su YP; Cheng TM; Shi CM A review of NIR dyes in cancer targeting and imaging. *Biomaterials* 2011, 32, 7127–7138. [PubMed: 21724249]
9. Formosinho SJ; Arnaut LG Excited-state proton transfer reactions II. Intramolecular reactions. *J. Photochem. Photobiol. A. : Chem* 1993, 75, 21–48.

10. Sedgwick AC; Wu L; Han HH; Bull SD; He XP; James TD; Sessler JL; Tang BZ; Tian H; Yoon J Excited-state intramolecular proton-transfer (ESIPT) based fluorescence sensors and imaging agents. *Chem. Soc. Rev* 2018, 47 (23), 8842–8880. [PubMed: 30361725]
11. Taki M; Wolford JL; O'Halloran TV Emission Ratiometric Imaging of Intracellular Zinc: Design of a Benzoxazole Fluorescent Sensor and Its Application in Two-Photon Microscopy. *J. Am. Chem. Soc* 2004, 126 (3), 712–713. [PubMed: 14733534]
12. Chu Q; Medvetz DA; Panzner MJ; Pang Y A fluorescent bis(benzoxazole) ligand: Toward binuclear Zn(II)-Zn(II) assembly. *Dalton Trans.* 2010, 39, 5254–5259. [PubMed: 20440438]
13. Xu Y; Pang Y Zinc binding-induced near-IR emission from excited-state intramolecular proton transfer of a bis(benzoxazole) derivative. *Chem. Commun* 2010, 46, 4070–4072.
14. Xu Y; Pang Y Zn<sup>2+</sup>-triggered excited-state intramolecular proton transfer: a sensitive probe with near-infrared emission from bis(benzoxazole) derivative. *Dalton Transactions* 2011, 40, 1503–1509. [PubMed: 21243147]
15. Xu Y; Liu Q; Dou B; Wright B; Wang J; Pang Y Zn<sup>2+</sup> Binding-Enabled Excited State Intramolecular Proton Transfer: A Step toward New Near-Infrared Fluorescent Probes for Imaging Applications. *Adv. Healthcare Mater* 2012, 1, 485–492.
16. Wang J; Pang Y A versatile synthesis of bis[2-(2'-hydroxyphenyl)benzoxazole] derivatives as zinc sensors. *RSC Advance* 2013, 3, 10208–10212.
17. Costa JCSD; Pais KC; Fernandes EL; Oliveira PSMD; Mendonca JS; Souza MVND; Peralta MA; Vasconcelos TR A. Simple reduction of ethyl, isopropyl and benzyl aromatic esters to alcohols using sodium borohydride-methanol system. *ARKIVOC* 2006, 128–133.
18. Boechat N; da Costa JCSD; Souza Mendonca JDS; Oliveira PSMD; Souza MVND A simple reduction of methyl aromatic esters to alcohols using sodium borohydride-methanol system. *Tetrahedron Lett.* 2004, 45 (31), 6021–6022.
19. Han SY; Lee HS; Choi DH; Hwang JW; Yang DM; Jun JG Efficient Total Synthesis of Piceatannol via (E)-Selective Wittig-Horner Reaction. *Synth. Commun* 2009, 39, 1425–1432.
20. Lee DH; Kim SY; Hong J-I A Fluorescent Pyrophosphate Sensor with High Selectivity over ATP in Water. *Angew. Chem. Int. Ed* 2004, 43 (36), 4777–4780.
21. Liu DJ; Credo GM; Su X; Wu K; Lim HC; Elibol OH; Bashir R; Varna M Surface immobilizable chelator for label-free electrical detection of pyrophosphate. *Chem. Commun* 2011, 47 (29), 8310–8312.
22. Knölker HJ; Fröhner W; Heinrich R Transition Metal Complexes in Organic Synthesis, Part 74: [1] Total Synthesis of the Marine Alkaloid 6-Chlorohyellazole. *Synlett* 2004, 15, 2705–2708.
23. Yoo WJ; Yuan H; Miyamura H; Kobayashi S Facile Preparation of 2-Substituted Benzoxazoles and Benzothiazoles via Aerobic Oxidation of Phenolic and Thiophenolic Imines Catalyzed by Polymer-Incarcerated Platinum Nanoclusters. *Adv. Synth. Catal* 2011, 353 (17), 3085–3089.
24. Wu IT; Chaing PY; Chang WJ; Sheu HS; Lee GH; Lai CK Columnar/smectic metallomesogens derived from heterocyclic benzoxazoles. *Tetrahedron* 2011, 67 (38), 7358–7369.
25. Chang J; Zhao K; Pan S Synthesis of 2-arylbenzoxazoles via DDQ promoted oxidative cyclization of phenolic Schiff bases—a solution-phase strategy for library synthesis. *Tetrahedron Lett.* 2002, 43, 951–954.
26. Varma RS; Kumar D Manganese triacetate oxidation of phenolic schiffs bases: Synthesis of 2-arylbenzoxazoles. *J. Heterocyclic Chem* 1998, 35 (6), 1539–1540.
27. Pawar SS; Dekhane DV; Shingare MS; Thore SN Alum (KAl(SO<sub>4</sub>)<sub>2</sub>·12H<sub>2</sub>O)-Catalyzed, Eco-Friendly, and Efficient One-Pot Synthesis of 2-Arylbenzothiazoles and 2-Arylbenzoxazole in Aqueous Medium. *Aust. J. Chem* 2008, 61 (11), 905–909.
28. Stephens FF; Bower JD The preparation of benzimidazoles and benzoxazoles from Schiffs bases. Part I. *J. Chem. Soc* 1949, 2971–2972.
29. Srivastava RG; Venkataramani PS Barium Manganate Oxidation in Organic Synthesis: Part III: Oxidation of Schiff's Bases to Benzimidazoles Benzoxazoles and Benzthiazoles. *Synth. Commun* 1988, 18 (13), 1537–1544.
30. Praveen C; Kumar KH; Muralidharan D; Perumal PT Oxidative cyclization of thiophenolic and phenolic Schiffs bases promoted by PCC: a new oxidant for 2-substituted benzothiazoles and benzoxazoles. *Tetrahedron* 2008, 64 (10), 2369–2374.

31. Tagawa Y; Koba H; Tomoike K; Sumoto K Synthesis of Caboxamycin and Its Derivatives Using Eco-Friendly Oxidation. *Heterocycles* 2011, 83 (4), 867–874.
32. Henderson SJ; Xia J; Wu H; Stafford AR; Leslie BA; Fredenburgh JC; Weitz DA; Weitz JI Zinc promotes clot stability by accelerating clot formation and modifying fibrin structure. *thrombosis and haemostasis* 2016, 115 (3), 533–42.
33. Hackley BM; Smith JC; Halsted JA A Simplified Method for Plasma Zinc Determination by Atomic Absorption Spectrophotometry. *Clin. Chem* 1968, 14, 1. [PubMed: 4965229]
34. Marx G; Korner G; Mou X; Gorodetsky R Packaging zinc, fibrinogen, and factor XIII in platelet  $\alpha$ -granules. *J. Cell. Physiol* 1993, 156 (3), 437–442. [PubMed: 8360253]
35. Tubek S; Grzanka P; Tubek I Role of Zinc in Hemostasis: A Review. *Biol. Trace Elem. Res* 2008, 121, 1–8. [PubMed: 17968515]
36. Mahdi F; Madar ZS; Figueroa CD; Schmaier AH Factor XII interacts with the multiprotein assembly of urokinase plasminogen activator receptor, gC1qR, and cytokeratin 1 on endothelial cell membranes. *Blood* 2002, 99 (10), 3585–3596. [PubMed: 11986212]
37. Vu TT; Fredenburgh JC; Weitz JI Zinc: An important cofactor in haemostasis and thrombosis. *Thromb Haemost* 2013, 109 (03), 421–430. [PubMed: 23306381]
38. Uppal R; Ciesinski KL; Chonde DB; Loving GS; Caravan P Discrete Bimodal Probes for Thrombus Imaging. *J. Am. Chem. Soc* 2012, 134, 10799–10802. [PubMed: 22698259]



**Highlights**

- Efficient synthesis for construction of a zinc probe
- Zinc binding to induce NIR emission from excited state intramolecular proton transfer
- NIR-emission with large Stokes shift
- Zinc binding response for thrombus imaging

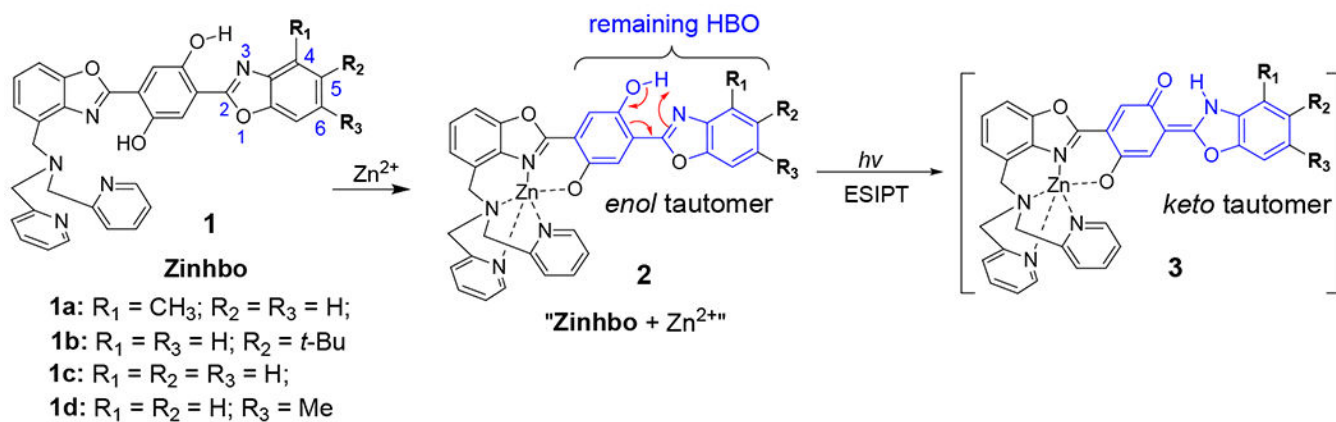


**Figure 1.** Chemical structure of Zinhbo compounds **1** as well as the *enol* and *keto* tautomer structures of the corresponding zinc complex.

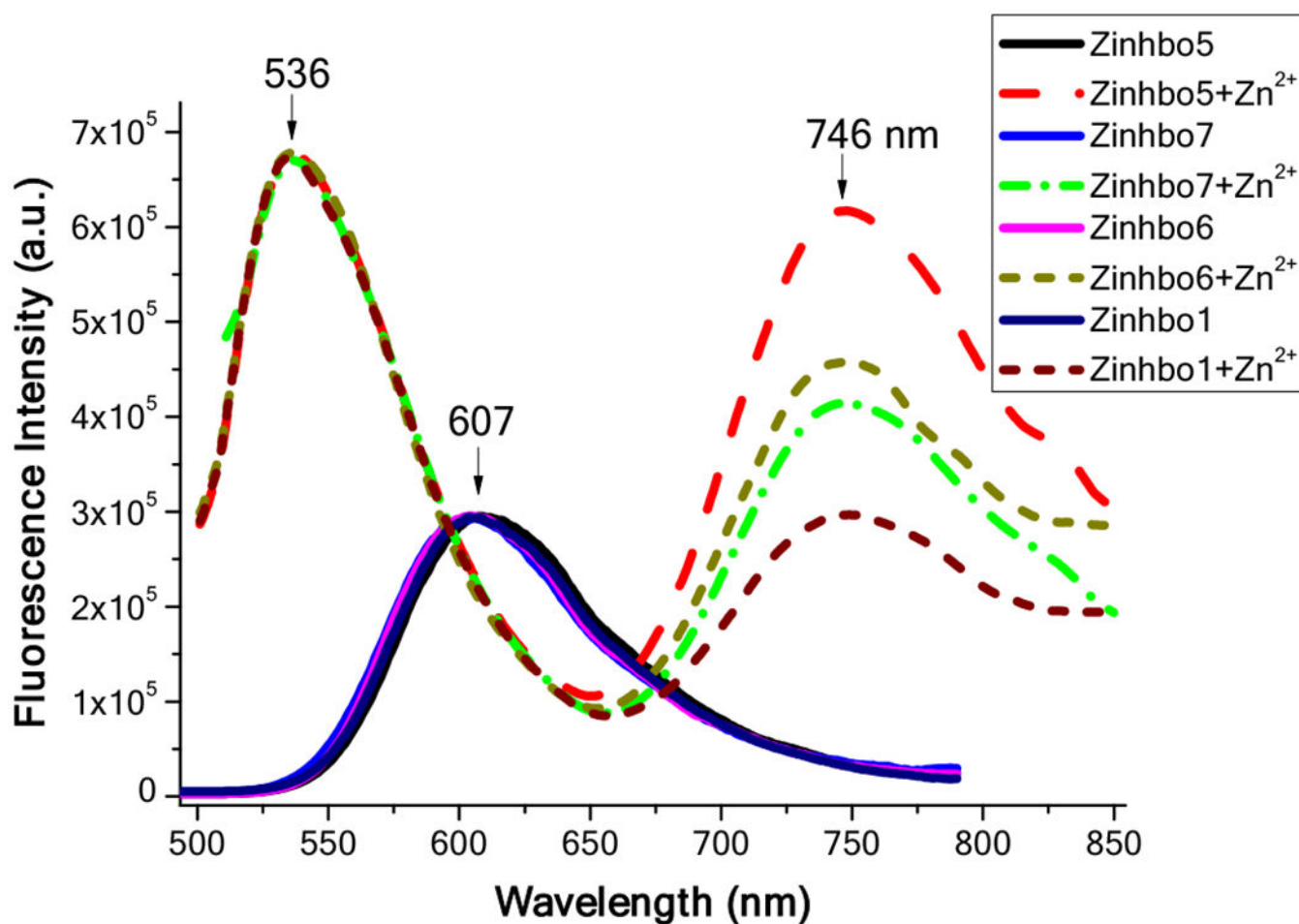


**Figure 2.** Normalized fluorescence spectra of Zinhbo compounds (5  $\mu\text{M}$ ; excitation at 414 nm) and Zinhbo- $\text{Zn}^{2+}$  complexes (formed upon addition of 1 equiv  $\text{Zn}^{2+}$ ) in  $\text{CH}_2\text{Cl}_2$  (excitation at 480 nm). The spectra are normalized at 607 nm for Zinhbo, and at 536 nm for Zinhbo- $\text{Zn}^{2+}$  complexes.

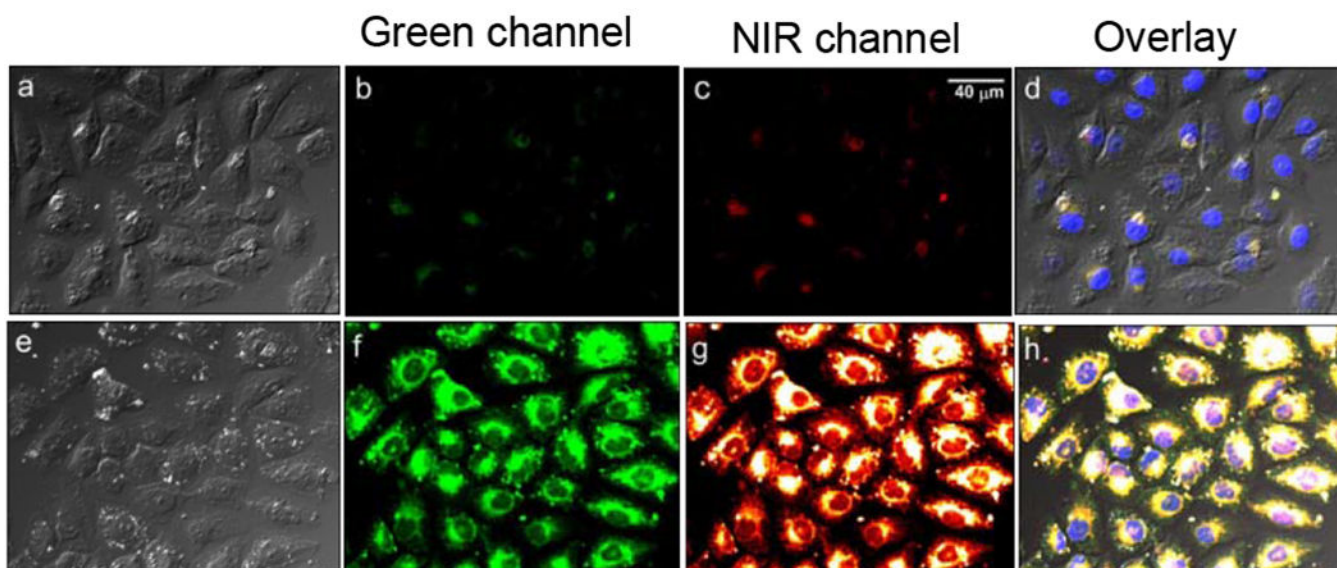


**Figure 3.**

Top: Fluorescence images of HeLa cells incubated with 10  $\mu\text{M}$  Zinhbo-5 for 60 min at 37°C in cell culture medium; Bottom: HeLa cells were first treated with 10  $\mu\text{M}$   $\text{Zn}^{2+}$  for 30 mins, washed 3 times with PBS, the cells were further incubated with 10  $\mu\text{M}$  Zinhbo-5 for another 60 min at 37°C in cell culture medium. The experiments were carried out on an Olympus FV1000 Confocal Microscopy, excited with a 488 nm laser, and the images were collected in both green channel (535-565 nm) and NIR channel (700-750 nm).

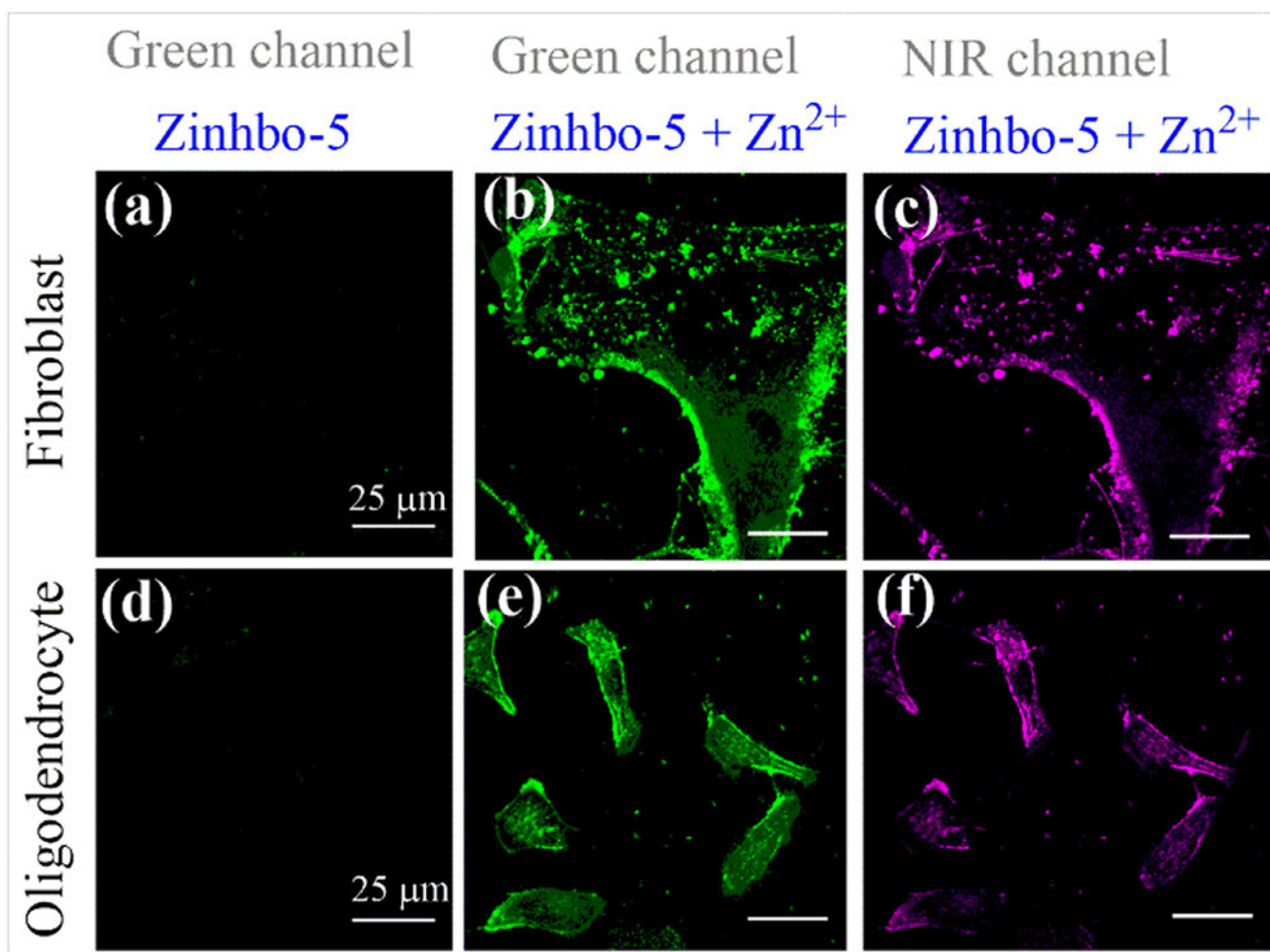


**Figure 4.** Confocal imaging of fibroblast (top row) and oligodendrocyte cells (bottom row) treated with TPEN (50  $\mu$ M), washed with cell medium, and incubated with Zinhbo-5 (5  $\mu$ M) for 30 min (images a & d; Ex/Em= 488/525 nm), followed by treatment with 50  $\mu$ M Zn<sup>2+</sup> for 30 mins in green channel (b and e, Ex/Em= 488/525 nm) and NIR channel (c and f; Ex/Em= 488/700 nm).

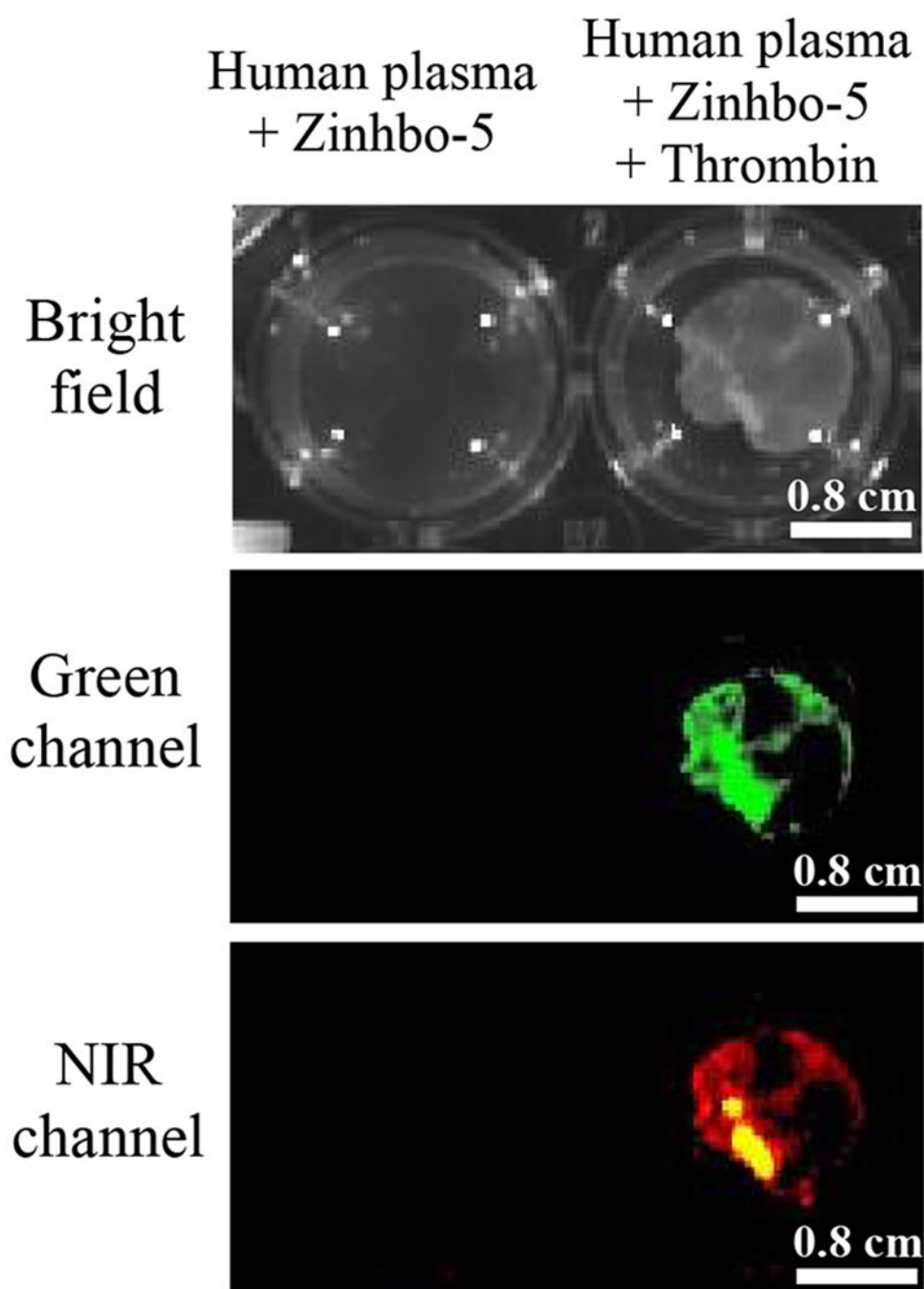
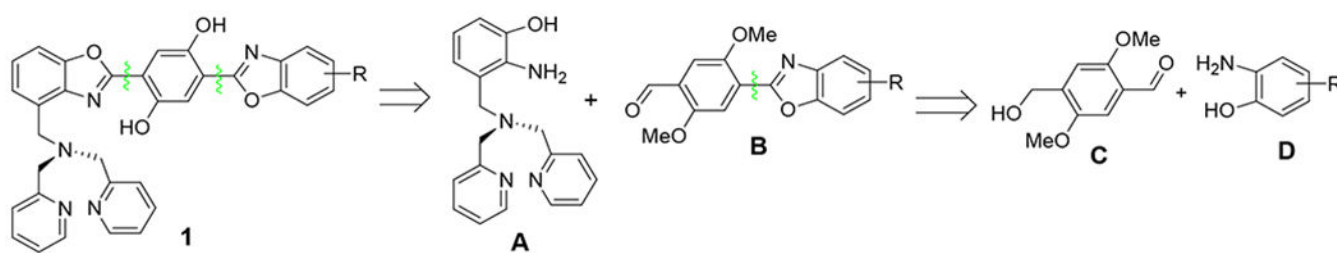
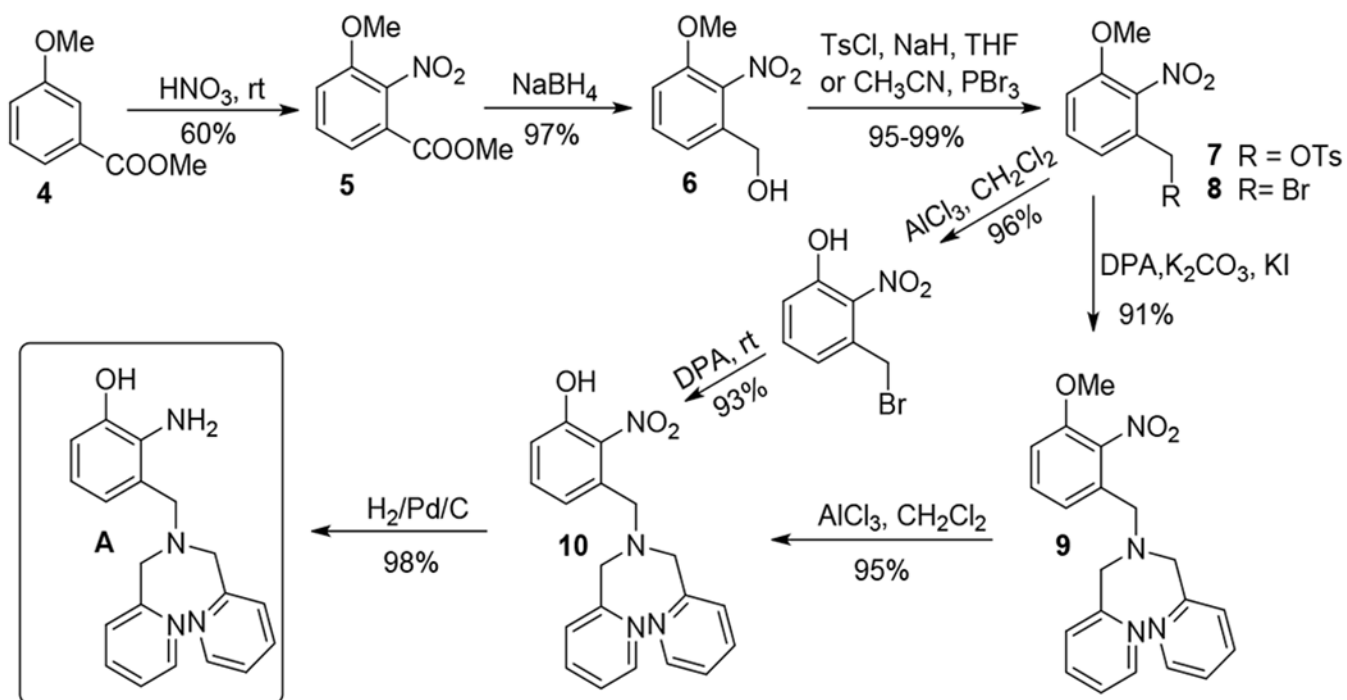


**Figure 5.**

*In vitro* NIR imaging of thrombus by using Zinhbo-5. Top row: Human plasma (0.5 mL) containing 1.0  $\mu$ M of Zinhbo-5 (left well); Human plasma containing 1.0  $\mu$ M of Zinhbo-5, followed by addition of 1.0  $\mu$ L of 1Unit/mL thrombin (right well, from Millipore Sigma, Cat. No. 605160). Middle and bottom rows: Human plasma and resulting clots were imaged with Ex/Em = 465/560 nm (Green channel) or Ex/Em = 465/760 nm (NIR channel) using an IVIS® Spectrum imaging system.

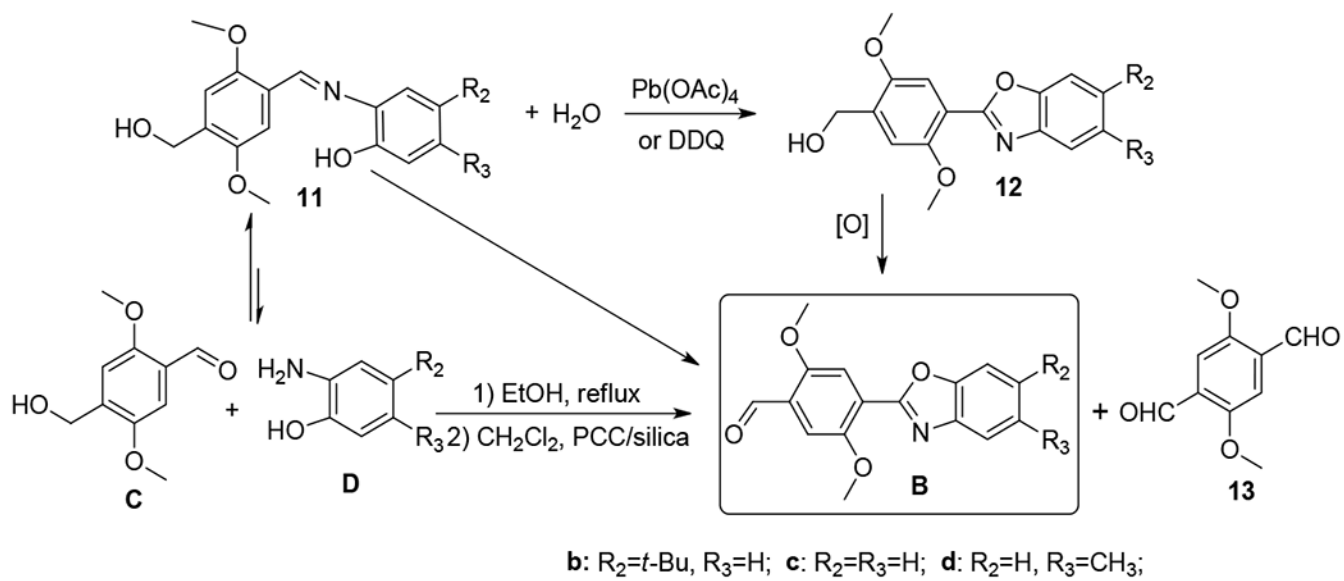


**Scheme 1.**  
Retrosynthetic analysis of the bis(HBO) derivatives.

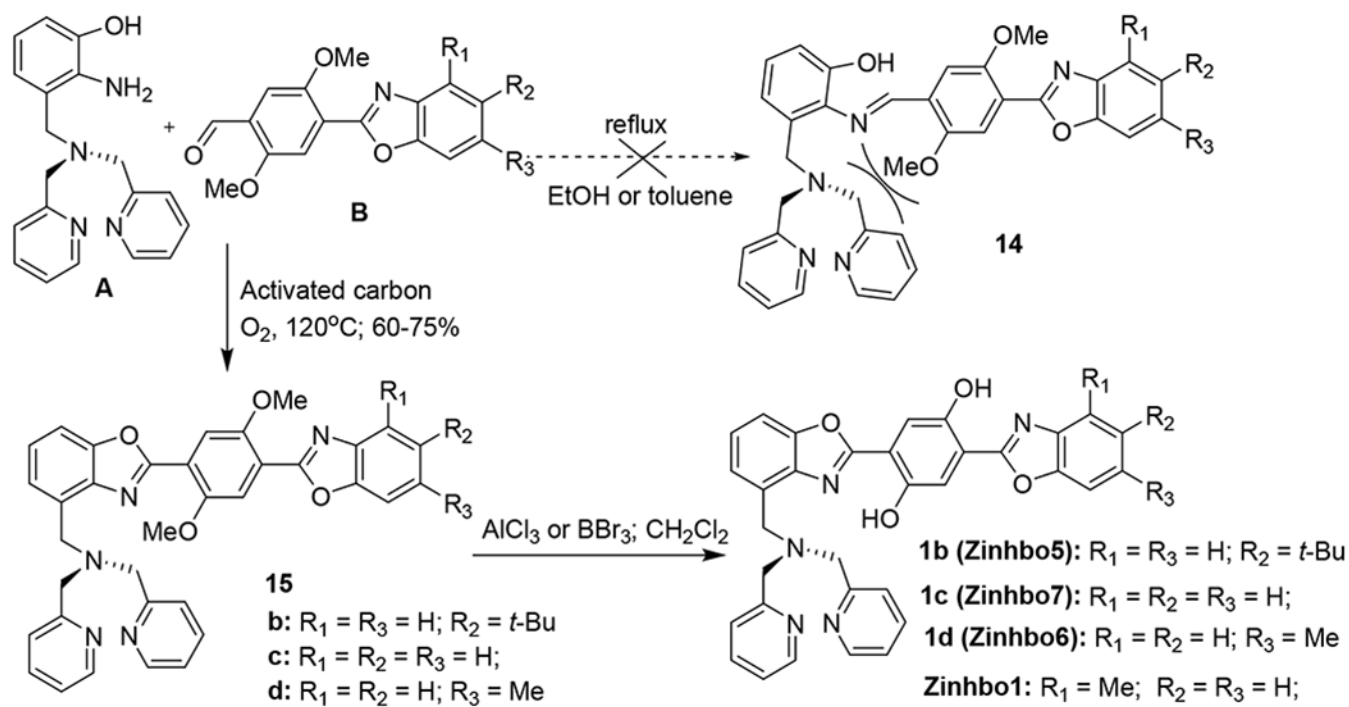


**Scheme 2.**  
Synthesis of key intermediate **A**.

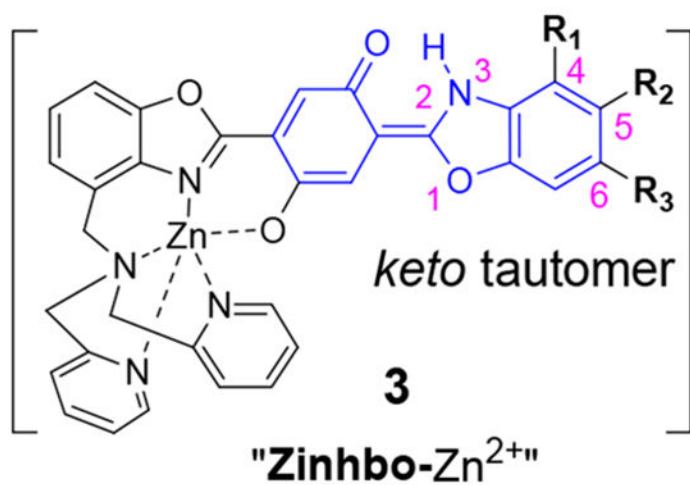




**Scheme 3.**  
Synthesis of key intermediate **B**.



**Scheme 4.**  
Construction of bis(HBO) system (Zinhbo dyes).

**Zinhbo1:**

Substituent		
R <sub>1</sub>	R <sub>2</sub>	R <sub>3</sub>
CH <sub>3</sub>	H	H
H	<i>t</i> -Bu	H
H	H	Me
H	H	H

**Zinhbo5:****Zinhbo6:****Zinhbo7:****Scheme 5.**Chemical structures of *keto* tautomer of Zinhbo-Zn complexes.